

Optimal Analysis of Seismic Response of a Tall Tower Monitored by an Integrated RTK-GPS System

**Xiaojing LI¹, Linlin GE², Eliathamby AMBIKAI RAJAH³,
Chris RIZOS⁴, and Yukio TAMURA⁵**

^{1,3} School of Electrical Engineering & Telecommunications

^{2,4} School of Surveying & Spatial Information Systems

The University of New South Wales

Sydney, NSW 2052 Australia

Email: xj.li@unsw.edu.au

⁵ Department of Architectural Engineering

Tokyo Polytechnic University

1583, Iiyama, Atsugi, Kanagawa, 243-0297, Japan

Abstract

Seismic response of a tall steel tower in Tokyo, Japan, has been monitored by an integrated RTK-GPS and accelerometer system and compared to results of finite element models (FEM) and frequency domain decomposition (FDD) method. The integrated results presented herein are consistent with FEM predicted values. Because of the inherent limitations of GPS and accelerometer when applied to civil structural monitoring, a solid reliability can only be realized through the multi-sensor integration. The integration enables system redundancy through information fusion by using digital signal processing techniques in the transformation of one form of measurement (e.g. displacement) to another (e.g. acceleration). Moreover, the newly developed algorithm for time-dominant frequency analysis presented in this paper supplies the frequency change information with respect to time. The findings have demonstrated the advantages of using high precision GPS sensor together with traditional accelerometer in civil structural monitoring under extreme loading conditions. The effectiveness of digital signal processing in optimal analysis of structural monitoring data from different sensors has been highlighted.

1. Introduction

Preliminary studies have proven the technical feasibility of using GPS and accelerometer to monitor dynamic structural deformation due to winds, traffic, earthquakes and similar loading events in, e.g., Hong Kong (Ding et al, 2002), UK (Ashkenazi and Roberts, 1997), USA (Kilpatrick et al, 2003), Singapore (Brownjohn et al, 1998) and Japan (Tamura et al, 2002). However, in current monitoring systems (Part 2) measurements from different sensors are usually analysed separately. There is much room for developing new methodologies to exploit the integrated monitoring system.

Advanced digital signal processing techniques provide us the possibility to reach the goal of a robust, high quality monitoring system through best utilizing the advantageous properties of each sensor. By analysing the spectrum of each sensor's measurements comprehensively (Part 3), the FEM predicted structural natural vibration frequency can be evaluated and any shift from the original frequency can also be detected. But usually such spectrum analysis gives no time information as to when the frequency shift occurs and hence what is the driving force. Applying the short time Fast Fourier Transform (FFT) through a new algorithm developed by the first author, the dominant frequency evolution along with time can be obtained (Part 4). Another significant improvement is that measurements can be transformed from one form to another using law of motion after digital filtering the original data (Part 5).

It is well known that light, flexible buildings are more favorable for resisting seismic force, while heavy, stiff buildings are more favorable for resisting wind force. Tall buildings in Japan have to satisfy these two opposite design criteria, and this is one of the most difficult design issues for tall buildings in Japan (Tamura, 2003). Measurement transformation has been successfully applied to data collected during a typhoon event by the authors in previous studies (e.g Li, 2004). Because earthquake induced structural response is very different from that due to typhoon, it is necessary to analyse the monitored seismic response as well in order to evaluate the reliability and robustness of the whole monitoring system

Through the results from analyzing data collected during the earthquake event, this paper will showcase the effectiveness of digital signal processing techniques in integrating RTK-GPS and accelerometer sensors for civil structural monitoring.

2. Information in RTK-GPS and Accelerometer Time Series Collected During the Earthquake

Figure 1 illustrates the experimental setup (Li, 2004) which has been used to monitor this 108m high steel tower continuously. Note the local monitoring-coordinate system was established so that X is East, Y is North, and Z is pointing to the Zenith. The RTK-GPS and accelerometer data were recorded at 10 Hz and 20 Hz sampling rates respectively. The reference point is 110m away from the tower in a 16m high rigid building. Data used in this study were collected from 18:00 to 19:00 JST when an earthquake event of magnitude Ms 7.0 occurred on 26 May 2003 at a depth of 71 km. Studies on a typhoon induced response of the tower has been published previously (Li, 2004). It would be interesting to compare and find the differences between earthquake and typhoon as to their effects on the structure.

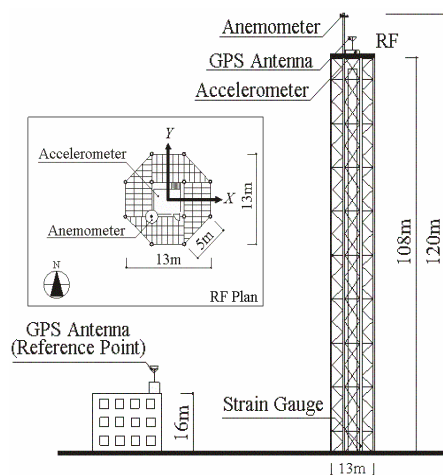


Figure 1 The 108m steel tower for GPS and accelerometer field experiment.

When an earthquake takes place, it causes two types of deformation: static and dynamic. The static deformation is represented by the cracks along the seismic fault. The dynamic motions are essentially sound waves radiated from the hypocentre as it ruptures. Two main waves are very important to be detected in real time, in order to mitigate the disaster caused by the quake. They are the first type of body waves named the **P wave** or **primary wave** which is the fastest seismic wave, and the second type of body waves called the **S wave** or **secondary wave** which is the second wave you feel in the earthquake. The P wave can move through solid rock and fluids. It pushes and pulls the rock as it moves through just like sound waves push and pull the air. An S wave is slower than a P wave and can only move through solid rock. This wave moves rock up and down, or side-to-side (Shearer, 1999). Due to different characteristics of sensors, the monitored structural response by RTK-GPS and accelerometer reveals different details, outlined below.

The overall two hour plots of RTK-GPS time series of displacements in X, Y and Z directions are shown in Figure 2. Measurements from the accelerometers (X and Y directions only) are given in Figure 3. Note the acceleration (Figure 3) has been limited to a period of 300 seconds in order to see both the P and S waves clearly. The peak-to-peak acceleration is almost 200cm/s^2 .

The least-squares polynomial fitting on GPS measurements can give us the static and semi-static displacements. The results from fitting (blue lines in Figure 2) show that maximum displacements in X and Y directions are all less than $\pm 1\text{cm}$ during the two hour period, indicating no significant static or semi-static movements. But in the Z direction the polynomial fit seems to suggest vertical ground movement of more than the $\pm 2\text{cm}$ GPS noise floor and the

peak-to-peak fluctuation also averaged over two centimeters after the 1500sec mark, probably due to surface waves induced by the strong earthquake.

Meanwhile, the S waves caused a peak-to-peak dynamic vibration of the tower of more than 6cm in the X and Y directions. However, P waves cannot be seen in the RTK-GPS time series (even when zoomed in). This is because the magnitude of P waves is 2-3 times smaller than the S waves and hence can be buried in the GPS noise. These P waves, however, can be recovered through double differentiating the GPS measured displacement and converting it to acceleration. No obvious dynamic movement was picked up in the Z direction when the seismic waves arrived due to the much higher noise level with the vertical component than with horizontal components.

From Figures 2 and 3, it can be seen that it is difficult to directly obtain the excited vibration frequencies from the time series. Both civil and earthquake engineers are interested in the seismic induced frequencies of the full-scale tower and need to know them accurately in order to compare with the originally designed free vibration frequency modes. Part 3 focuses on this.

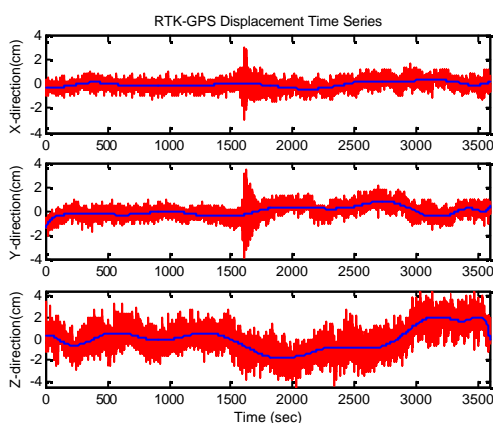


Figure 2 RTK-GPS measured displacements.

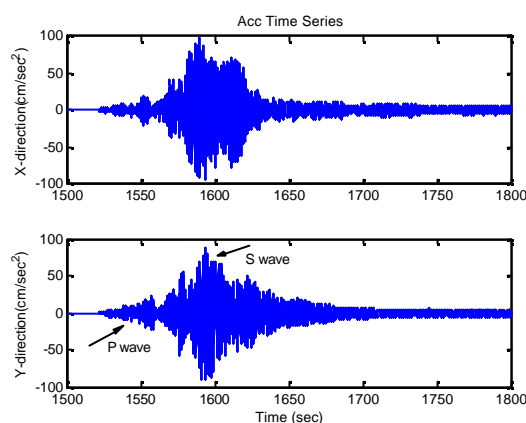


Figure 3 Acceleration time series measured by accelerometers.

3. Vibration Signals obtained from traditional “global” FFT analysis

It is possible to assess the accuracy of recorded data by analysing the spectrum of the seismic induced vibration of the tower. The Fast Fourier Transform (FFT) yields the spectrum of RTK-GPS measurements (Figure 4). Studying the three spectrums closely by zooming in, e.g. as given in Figure 5, it is obvious that the largest amplitude at 0Hz presents a strong static movement. And semi-static movements, centred at 0.13Hz and ranging from 0.05 to 0.2Hz, are contributing to all three components. This could be multipath effects combined with semi-static movements. It has been suggested that 0.05-0.2Hz is the spectrum range of multipath through analysing the wind speed fluctuation in the typhoon event (Li, 2004). In the meantime, both X and Y directions show peaks at 0.57Hz and 2.16Hz. There is no clear peak in the Z direction at the expected signals, but signal or noise at the lower frequency end (0-0.8Hz) is much stronger than in the other two directions. This can be partly explained as the static and semi-static

movements during the quake affected the tower mostly along the Z direction. This agrees with the time series shown in Figure 2.

The accelerometer's performance in the seismic event is analysed in the same way. Figure 6 is the FFT spectrum of accelerometer measurements. There are three peaks all in the same locations in the X and Y directions, of which the 0.57Hz and 2.16Hz peaks are identical to the GPS spectrum, while the 4.58Hz as a high order harmonic cannot be identified with confidence from the spectrum of GPS. A very clear difference between the spectrums of the two sensors is that accelerometer spectrums do not contain static and semi-static components at all.

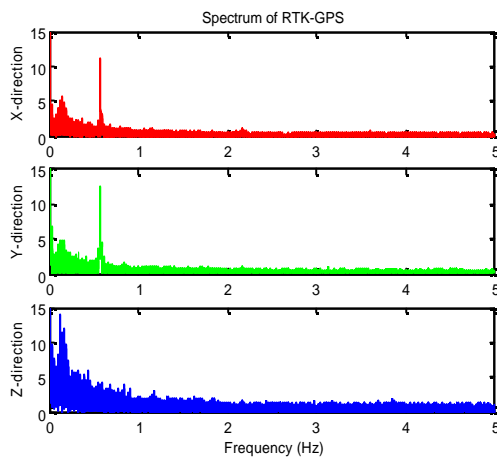


Figure 4 FFT spectrums of GPS.

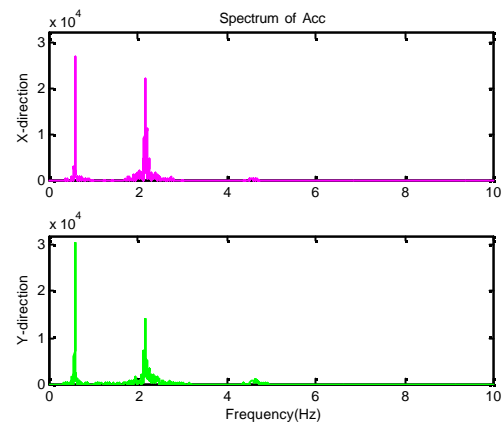


Figure 6 FFT spectrum of the acceleration.

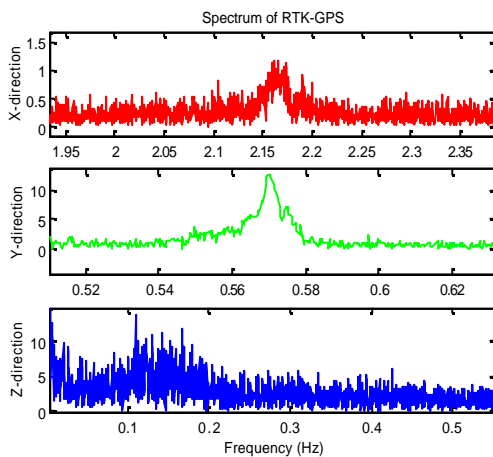


Figure 5 Zoom-in FFT spectrums of GPS.

It is clear that the spectrums for both the accelerometer and RTK-GPS have the frequency of 0.57Hz, indicating that it is the lowest natural frequency of the steel tower. This result agrees with Tamura et al (2002), using the power spectral density analysis to process the typhoon event data in 10 min mean. FEM and FDD analysis have also confirmed that 0.57Hz is the first mode natural frequency of the tower, 2.15Hz and 4.48Hz are the 2nd mode and 3rd mode respectively for FEM modeling, although these are slightly higher with the FDD method, i.e. 2.18Hz and 4.58Hz (Yoshida et al, 2003). Hence the 2.16Hz and 4.58Hz from practical full-scale measurements are the 2nd and 3rd mode natural frequencies of the tower. Despite of this good agreement, from the traditional FFT it is not possible to tell when the vibrations of different frequencies are excited, i.e. the crucial time information is missing. This shortcoming will be partially addressed in Part 4.

4. Dominant Frequency Signals Obtained From Short Time FFT Analysis

Traditional FFT spectrum represents the frequency composition of the WHOLE time series. It tells the relative strength (amplitude) of the frequency components, but does NOT tell when a particular frequency component occurs or takes over as the most significant frequency. It might be very useful to assess the response of or damage to the structure if it can be detected when a particular frequency component becomes dominant. One way of determining this frequency-time relationship is to apply the FFT to a short segment of the time series each time and to focus on the strongest peak in the spectrum. Thus the time and dominant frequency relationship is established.

Consider the measured digital signal of $x[n]$ as a time series with respect to t . The spectrum $X[f_a]$ obtained by using Fourier transform of a discrete signal (DTFT) is a function of t , which can be derived as follows. First, Fourier transform of a discrete signal (Ambikairajah, 2003) is:

$$X[\mathbf{q}] = \sum_{n=-\infty}^{\infty} x[n]e^{-j\mathbf{nq}}, \quad -\mathbf{p} \leq \mathbf{q} \leq \mathbf{p} \quad (1)$$

Where, $\mathbf{q} = \mathbf{w}T$ is the relative frequency, T is sampling period, and \mathbf{w} is the frequency of the signal in radians.

Considering f_a is the frequency of the signal, and $\mathbf{w} = 2\mathbf{p}f_a$. The sampling frequency is determined as $f_s = \frac{1}{T}$. Therefore, \mathbf{q} can be given by:

$$\mathbf{q} = 2\mathbf{p} \frac{f_a}{f_s} \quad (2)$$

Then, the time length t of the measurements can be calculated by using the sampling period T multiply the numbers of samples n .

$$t = nT, \quad -\infty \leq n \leq \infty \quad (3)$$

Substituting Eq. (1) with (2) and (3), Eq. (1) can be rewritten as:

$$X[f_a] = \sum_{n=-\infty}^{\infty} x[n] e^{-jn2\pi \frac{f_a}{f_s}} = \sum_{n=-\infty}^{\infty} x[n] e^{-j2\pi f_a t}, \quad -\frac{f_s}{2} \leq f_a \leq \frac{f_s}{2} \quad (4)$$

Hence, from Eq. (4) we can see that the frequency f_a of the digital signal $x[n]$ is a function of time t . When t approaches zero, the output frequency from DTFT becomes the instantaneous frequency. In other words, by applying DTFT on small samples of measurements, the time-frequency relationship can be established. The instantaneous frequency output can be expressed as:

$$X[f_a] = \sum_{n=0}^N x[n] e^{-jn2\pi \frac{f_a}{f_s}}, \quad (5)$$

The obvious approach is to segment the samples into smaller frames, then apply FFT to each frame in turn. Truncating the sampled signal into the N -sample record is equivalent to multiplying it by a rectangular window of width $\Delta t = NT$ (Mulgrew et al, 1999). This ‘‘Windowing’’ process introduces a slight distortion into the frequency representation of the signal being analysed. This windowing process is non-avoidable, because we can never have access to an infinite data record. However it can be improved by choosing an appropriately tapered window.

In order to have a digital frequency output in discrete form, sample the continuous f_a in N equally spaced interval, the obtained frequency resolution Δf_a is:

$$\Delta f_a = \frac{f_s}{N} \quad (6)$$

From Eq. (6) obviously the frequency resolution (spacing in Hz) between the discrete Fourier transform (DFT) values is dependent on the number of samples. Larger number of samples will give a higher frequency resolution. But the time resolution Δt is just the opposite, i.e. larger number of samples will lead to lower time resolution.

Now we apply Eq. (5) to analyse the tower’s frequency response with respect to time during the earthquake event. To represent the typical frequency which appeared in the FFT spectrum with an appropriate frequency and time resolution, it is important to select appropriate window length of measurements to be analysed each time, and only the maximum peak will be taken into account. Figure 7 is the result for GPS measurements in Y direction clearly showing the abrupt frequency shift. A total of 256 samples were processed each time. Hence the time length is 25.6s. It can be seen clearly that the tower experienced the strongest vibration lasting for about 7 minutes around 18:30 when the tower’s first order natural frequency 0.57Hz became dominant. This cannot be determined from the GPS displacement time series itself because it is too noisy (cf. Figure 2).

It is interesting to see that this duration estimated from accelerometer measurement in Y direction is about 14 minutes, as shown in Figure 8. Please note that the starting time for 0.57Hz signal is the same for both GPS and accelerometer. The finishing time is different because the amplitude of seismic waves decreases gradually and when the induced displacement is smaller than the RTK-GPS noise floor it cannot be tracked by GPS anymore. The seismic induced acceleration, however, will continue to be tracked by the accelerometer for as long as 0.57Hz is

dominant. Because acceleration measurements were obtained at the sampling rate of 20Hz, using the same window length of 256 samples, the frequency resolution is half of that for displacement measured by GPS while the time resolution is twice higher.

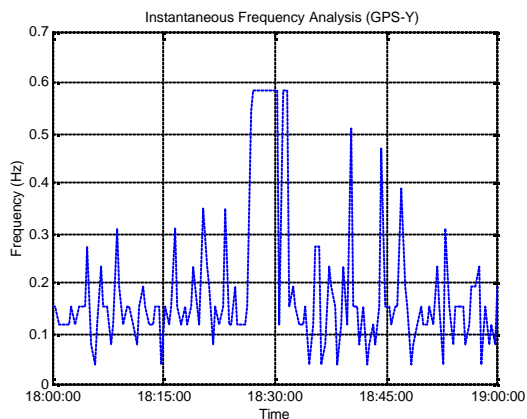


Figure 7 Frequency evolution on GPS y-direction

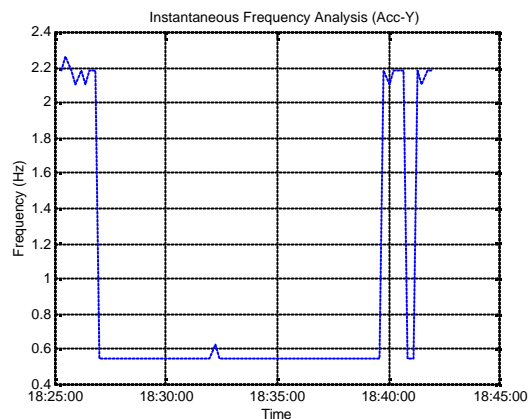


Figure 8 Frequency evolution on Acc y-direction.

Structural response is very complicated. Even in a very short time segment the appeared spectrum is not of a single frequency due to its non-stationary features caused by fluctuations of driving force. There is a bandwidth for each central frequency at the natural vibration mode in the global FFT spectrum as well. If we take more frequencies into account in the frequency evolution analysis, the frequencies forming the “band” would be revealed clearly. Figures 9 and 10 are results when up to three major frequencies are considered for GPS and accelerometer measurements in Y direction respectively. These two figures were generated using the window length of 256 samples as well and focused on the period of the earthquake.

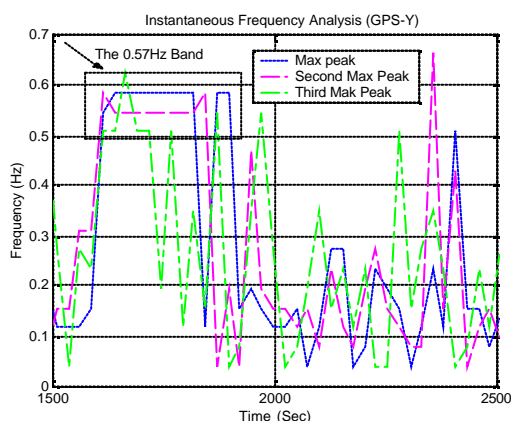


Figure 9 Frequencies evolution on GPS Y-direction.

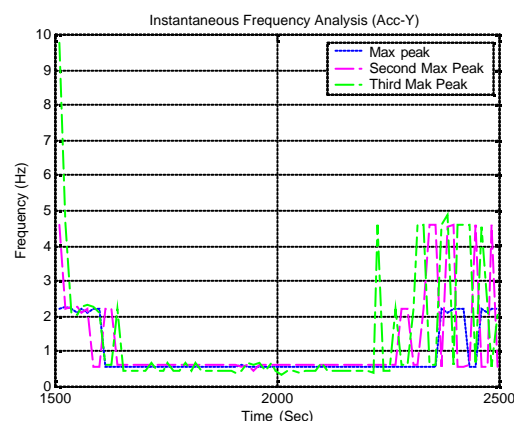


Figure 10 Frequencies evolution on Acc Y-direction.

5. Information Fusion Through Measurements Combination and Transformation

From the above signal analysis, the GPS sensor gives more information at the low frequency end (static and semi-static) while the accelerometer sensor gives more at the high frequency end (dynamic). This means that both of them lose information which is very important for civil engineers in evaluating the deformation of a structure. The following analysis will attempt to address this problem

First, a double differentiation procedure is applied to a segment of RTK-GPS measured displacement data (Y direction) of 200 second duration in order to convert them into acceleration. Figures 11 shows the results of acceleration derived from RTK-GPS measured displacement, compared to accelerometer-measured acceleration. In the figure, the upper plot is the GPS displacement; the middle plot is the acceleration derived from the GPS measurements; and the bottom plot is the accelerometer-measured acceleration. Comparing the time series in the middle and bottom plots, it can be seen that they agree well with each other, although the converted acceleration time series shows high frequency fluctuations due to GPS-specific noise. It is also interesting to see that the P and S seismic waves are clearly visible in the horizontal directions from the accelerometer data. However, these waves (especially the P waves) are not so obvious from the original GPS displacement time series. After the double differentiation, the accelerations derived from RTK-GPS also show clearly the seismic waves. Therefore, GPS can be used as a seismometer (Ge, 1999).

In the reverse data processing of Figure 11, the upper plot in Figure 12 is displacement directly measured by GPS and bottom plot is displacement derived from accelerometer data through double integration. Results of their polynomial fitting are given as well. From the results shown in Figure 12, it can be seen that in the dynamic part during the quake the two agree very well with each other. However, significant differences can be seen in the part measured shortly before the quake because the static and quasi-static displacements are missing from the accelerometer derived results.

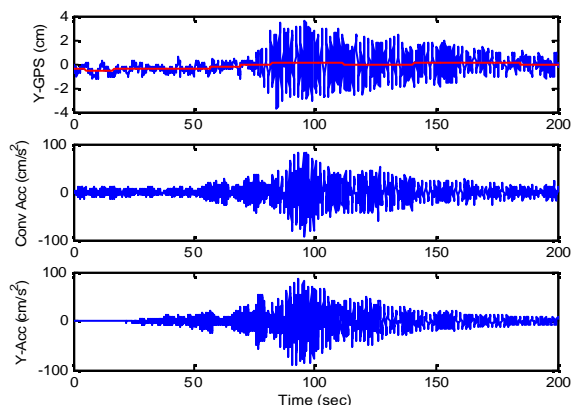


Figure 11 Comparison between RTK-GPS derived and accelerometer-measured accelerations (Y-direction).

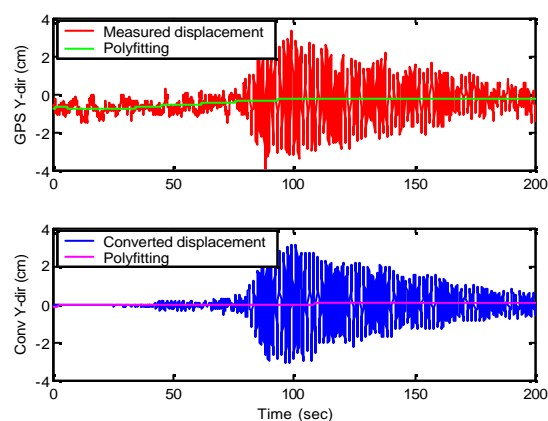


Figure 12 Comparison between RTK-GPS measured and accelerometer derived displacements (Y-direction).

In order to compare monitoring results directly and to deal with the unexpected data loss especially with RTK-GPS, it is essential to transform the measurements faithfully from one form (e.g. acceleration) to another (e.g. displacement). There is no way to directly transform the measurements by a simple mathematical function, because RTK-GPS is good at monitoring static and lower frequency components while the accelerometer is better with dynamic high frequency component. GPS measurements are also contaminated by multipath. Thus filtering techniques have to be applied in pre-processing. Moreover, time delay and phase lag caused by filtering need to be compensated. Figures 13 and 14 are the zoom-in on a segment of Figures 11 and 12 respectively. These figures give fine details and support earlier discussions on information fusion for the integrated monitoring system.

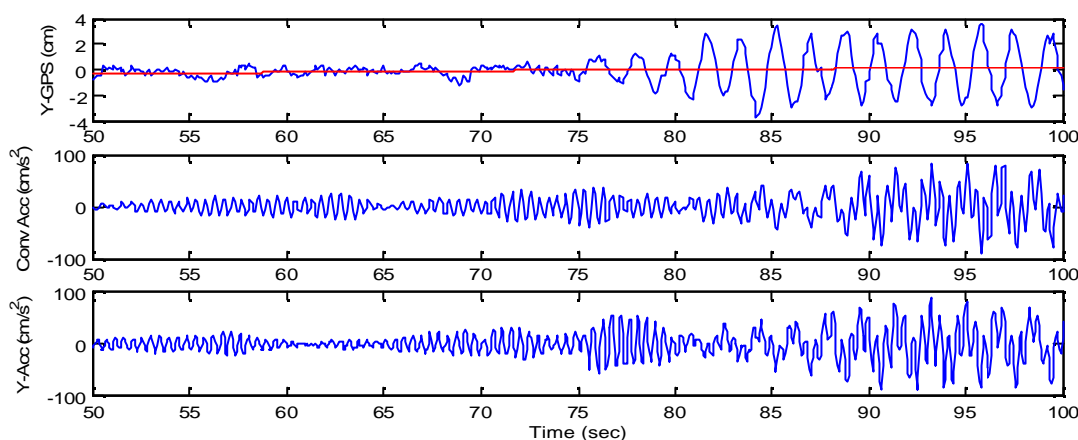


Figure 13 A segment of Figure 11.

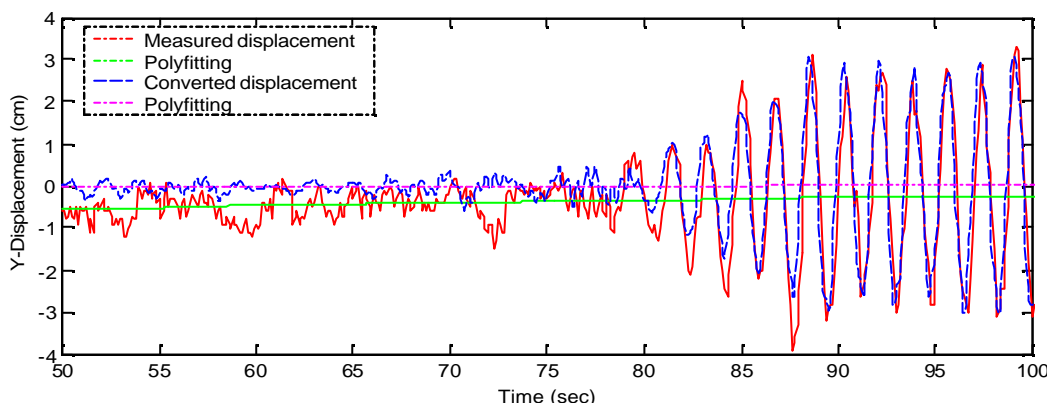


Figure 14 A segment of Figure 12.

6. Concluding Remarks

GPS and accelerometer sensors have been installed on a 108m tall steel tower and data have been collected at 10Hz and 20Hz respectively during the Ms 7.0 earthquake on 26 May 2003. The

earthquake induced responses of the tower have been analysed in both the time and frequency domains. In the frequency domain, both the GPS and accelerometer results show strong peaks at 0.57Hz, which agrees with previous studies using different methods with typhoon induced responses and the FEM and FDD analysing results, although GPS measurements are noisy in the low frequency end. Short time FFT has been successfully applied to establish the frequency evolution, not only for the dominant frequency but also for another two major frequencies. Measurements have been converted to displacement (in the case of accelerometer) and acceleration (in the case of GPS) through double integration and double differentiation respectively, for the purpose of direct comparison and data fusion. The results agree with each other very well, except that the static component is missing from the accelerometer derived results. The benefits of an integrated GPS and accelerometer system to monitor structural deformation have been highlighted. Digital signal processing techniques do provide opportunities to significantly improve the performance of the whole monitoring system.

Acknowledgements

The first author wishes to thank the Faculty of Engineering of UNSW for the scholarship supporting her PhD studies. The research is sponsored by a Faculty Research Grant of the UNSW.

REFERENCES

- Ambikairajah, Associate Professor E., 2003. Lecture. School of Electrical Engineering & Telecommunications, the University of New South Wales, Australia.
- Ashkenazi, V., & Roberts, G.W., 1997. Experimental monitoring of the Humber Bridge using GPS, *Proc. of Institution of Civil Engineers*, 120, 177-182.
- Brownjohn, J., Pan, T.C., Mita, A., & Chow, K.F., 1998. Dynamic and static response of Republic Plaza, *Journal of the Institution of Engineers Singapore*, 38(2) 35-41.
- Ding, Xiao-Li, Huang, D.F., Yin, J.H., Chen, Yong-Qi, Lau, C.K., Yang, Y.W. And Sun, Y.R. (2002). A New Generation of Multi-Antenna GPS System for Landslide and Structural Deformation Monitoring. In ANSON, M., KO, J.M. and LAM, E.S.S., eds., *Advanced in Building Technology*, Elsevier, Hong Kong, pp. 1611-1618.
- Ge, L., 1999. GPS seismometer and its signal extraction, *Proc. Satellite Division of the Institute of Navigation 12th International Technical Meeting*, September 14-17, Nashville, Tennessee, USA, 41-51.
- Kilpatrick, J., Kijewski, T., Williams, T., Kwon, D.K., Young, B., Abdelrazaq, A., Galsworthy, J., Morrish, D., Isyumov, N., & Kareem, A., 2003. Full scale validation of the predicted response of tall buildings: preliminary results of the Chicago monitoring project, *Proc. 11th Intern. Conf. on Wind Engineering*, June 2-5, Lubbock, Texas, USA.
- Li, X, 2004. The Advantage of an Integrated RTK-GPS System in Monitoring Structural Deformation, *Journal of Global Positioning Systems*, Vol.3, No. 1-2: 191-199.
- Mulgrew, B., P. Grant and J. Thompson, 1999. *Digital Signal Processing - Concepts and Applications*, Macmillan: Basingstoke, 356pp.
- Shearer, P., 1999. *Introduction to seismology*, New York: Cambridge University Press, 260pp.

- Tamura, Y., Matsui, M., Pagnini, L.-C., Ishibashi, R., & Yoshida, A., 2002. Measurement of wind-induced response of buildings using RTK-GPS, *J. Wind Eng. and Industrial Aerodynamics*, 90, 1783-1793.
- Tamura, Y., 2003. Design issues for tall buildings from acceleration to damping. *The 11th International Conference on Wind Engineering (11 ICWE)*, Lubbock, Texas, USA, June 2-5.
- Yoshida, A., Tamura, Y., Matsui, M., & Ishibashi, S., 2003. Integrity monitoring of buildings by hybrid use of RTK-GPS and FEM analysis, *1st International Conference on Structural Health Monitoring and Intelligent Infrastructure*, November 13-15, Tokyo, Japan.